Supplement of Atmos. Chem. Phys., 24, 12295–12321, 2024
https://doi.org/10.5194/acp-24-12295-2024-supplement

Supplement of

Particulate emissions from cooking: emission factors, emission dynamics, and mass spectrometric analysis for different cooking methods

Julia Pikmann et al.

Correspondence to: Frank Drewnick (frank.drewnick@mpic.de)

S1 Calculation of mass concentrations

For calculation of the mass concentrations of PM_1, $PM_{2.5}$, and PM_{10} in a first step the particle number size distributions measured with the FMPS (d_p = 5.6 – 560 nm) and OPC (d_p = 0.25 – 32 µm) were combined. To this end, the OPC data were re-binned from optical to geometric particle diameters before merging them with the FMPS data. For the Christmas market data, we assumed for the optical particle properties values for a semi-urban aerosol, based on literature values: For fine particles (d_p < 700 nm), we assumed a mixture of organics, ammonium chloride, ammonium sulfate, and ammonium nitrate with refractive indices of or close to 1.55 (Levin et al., 2010; Tang, 1996), and for coarse particles (d_p > 3000 nm), we assumed a mixture of mineral dust and sea salt with refractive indices of 1.56-i.006 (Seinfeld and Pandis, 2006) and 1.544 (Hinds, 1999), respectively. For particles in the intermediate size range, a mixture of both particle types was assumed, with log-linearly interpolated particle numbers of the fine and coarse particles. For the laboratory cooking experiments, we supposed that the fine particles consisted mostly of rapeseed oil, the used oil for cooking, with a refractive index of 1.47 (Rumble, 2022) and within the coarse particles, 5% by particle number were assumed to be of salt and the remainder oil. For the Christmas market data, we assumed for the coarse particles a particle number fraction of 0.9 for mineral dust and 0.1 for sea salt. The necessary Mie scattering curves for the different particle types, which were used for the conversion of optical into geometric particle diameters, were calculated using an in-house tool (Vetter, 2004) applying the measurement geometry in the OPC, i.e. a refractive index of 1.588 of the calibration particles (PSL), a scattering angle of 60° to 120°, a laser wavelength of 655 nm, and a distance of the detector to the scattering volume of 1.5 cm (Vetter, 2004).

Since we found that the FMPS under-measures the concentrations in the uppermost size channels, these were corrected using the lower OPC size channels.

To calculate the mass concentrations from the resulting merged size distributions, different densities were used for different particle types assuming spherical particles. The densities for salt and mineral dust were assumed to be 2.17 g cm^{-3} (Baron et al., 2011) and 2.7 g cm^{-3} (Hinds, 1999; Reitz, 2011), respectively. The density for fine particles was calculated using the AMS and black carbon data based on the equation of Salcedo et al. (2006) for the overall density and Kuwata et al. (2012) for the density of organics. In this process, only data points were considered with AMS-measured organic mass concentrations above 1 µg m^{-3}.

The uncertainty for the mass concentrations was estimated to be 34%, based on error propagation from the uncertainty from the merging of the FMPS and OPC data (30%) and the uncertainty of the density (15%).

S2 PMF data analysis

As described in Pikmann et al., SI (2022), “for PMF analysis of the organic aerosol, the high-resolution data with error matrix were prepared with PIKA 1.23I. Ions with signal-to-noise ratio (SNR) < 2 were down weighted through increase of the corresponding error by a factor of 2, while ions with SNR < 0.2 were discarded from the data. The CO_2^+ ion and related ions (*m/z* 16, 17, 18 and 28) were down weighted by a factor of SQRT(5) as they all contain the same information. Additionally, “noisy” ions without contribution to the total measured signal were discarded. To find a robust solution the analysis was run for 1 to 7 factor solutions, with fpeak -1 to 1 (steps of 0.1) and seed 0 to 50 (steps of 1).” The chosen three-factor solutions were for fpeak = 0 and seed = 2 for Ingelheim and seed = 8 for Bingen. Solutions with more factors resulted in splitting of factors, generating factors which were physically meaningless. The PMF solutions were assigned to aerosol types through comparison of the factor mass spectra with literature references and of the factor time series with the data from other instruments. The uncertainty of the time series (Δ_{TS}) and mass spectra (Δ_{MS}) for the chosen solution was estimated using two methods: 1. the bootstrap method (Ulbrich et al., 2009); 2. by calculating the standard deviation for each time step resp. *m/z* from the set of all physically meaningful solutions obtained by variation of the fpeak and seed value as shown in Eq. (S1) and (S2) (Freutel et al., 2013).

$$\Delta_{TS} = \frac{\sum_{i=1}^{n} \frac{\sigma_{p,i}}{\bar{x}_{p,i}}}{n} \quad \text{(S1)}$$

$$\Delta_{MS} = \frac{\sum_{i=1}^{n} \sigma_{p,i}}{\sum_{i=1}^{n} \bar{x}_{p,i}} \quad \text{(S2)}$$

n is the number of *m/z* or time intervals, $\bar{x}_{p,i}$ and $\sigma_{p,i}$ are the average and standard deviation for one *m/z* or time interval, respectively. The uncertainty was in the order of 20 – 30%.

S3 Uncertainty calculation of RIE_{COA} values

The uncertainty of the RIE_{COA} value was calculated using multiplicative uncertainty propagation from the uncertainty of the PM_1 mass concentration based on the FMPS and OPC data (PM_1) and the PM_1 mass concentration from the AMS and BC measurements ($PM_{1,AMS+BC}$). This calculation is based on the method of Katz et al. (2021).

The uncertainty of PM_1 is dependent on the uncertainties of the calculated density and of the PM_1 volume and amounts to 34% (see Sect. S1). For the uncertainty of $PM_{1,AMS+BC}$ only the measured organics fraction (M_{Org}) is considered, as the inorganics and BC concentrations were negligible. The uncertainty of the organics mass fraction is dependent on the uncertainty of the measured instrument flow rate Q_{AMS} ($\Delta Q_{AMS} = 10\%$) and the uncertainty of the calibrated ionization efficiency IE_{NO_3} ($\Delta IE_{NO_3} = 15\%$) resulting in 18% total uncertainty (Eq. (S3) and (S4)) assuming CE = 1 without any uncertainty.

$$M_{Org} \sim \frac{1}{Q_{AMS}} * \frac{1}{IE_{NO_3}} \quad \text{(S3)}$$

$$\Delta M_{Org} = \sqrt{0.1^2 + 0.15^2} = 0.18 = 18\% \quad \text{(S4)}$$

The total uncertainty for RIE_{COA} amounts to 38% (Eq. (S5)).

$$\Delta RIE_{COA} = \sqrt{0.18^2 + 0.34^2} = 0.38 = 38\% \quad \text{(S5)}$$

S4 Additional figures and tables

Table S1: List of prepared dishes and the amounts of individual ingredients.

Dish	Preparation method	Ingredients
Fried potatoes	Stir-frying	1 kg potatoes (unpeeled, sliced) ~6 tbsp rapeseed oil (for frying)
Bratwurst	Stir-frying	4 bratwurst (total 600 — 640 g) ~2 tbsp rapeseed oil (for frying)
Schnitzel	Stir-frying	4 schnitzel (total 680 — 760 g) ~8 tbsp rapeseed oil (for frying)
Fish	Stir-frying	2.5 whole trouts (total 800 — 1200 g) Flour for breading ~6 tbsp rapeseed oil (for frying)
Spaghetti Bolognese	Stir-frying	400 g ground beef 250 g spaghetti 1 carrot 175 g celery 1 onion 2 garlic cloves 800 g tomatoes (canned) 20 g fresh basil ~4 tbsp rapeseed oil (for frying) Condiments: dried oregano, dried thyme, dried bay leaf
Stir-fried vegetables	Stir-frying	2 onions 2 bell peppers 6 tomatoes 1 zucchini 250 g champignons 2 garlic cloves 20 g fresh basil 200 g cream ~4 tbsp rapeseed oil (for frying) Condiments: paprika

(continued on next page)

Table S1: List of prepared dishes and the amounts of individual ingredients. (continued)

Dish	Preparation method	Ingredients
Indian curry	Stir-frying	420 g chicken breast 240 g chickpeas (canned) 2 carrots 2 red onions 30 g ginger 2 garlic cloves 400 mL coconut milk ~4 tbsp rapeseed oil (for frying)
Boiled potatoes	Boiling	1 kg potatoes in salted water (unpeeled, whole)
Rice	Boiling	250 g rice in salted water
Noodles	Boiling	250 g spaghetti in salted water
Bavarian doughnut (in pot)	Deep-frying	Dough prepared from: 125 mL milk 100 g butter 500 g wheat flour 7 g dried yeast 30 g sugar 8 g vanilla sugar 2 eggs 1.5 L rapeseed oil for frying
French fries (pot)	Deep-frying	1 kg French fries (frozen) 2.5 L rapeseed oil for frying
French fries (deep fryer)	Deep-frying	1 kg French fries (frozen) 2.5 L rapeseed oil for frying
Pizza	Baking	3 salami pizza (frozen, total 960 g)
Baked potatoes	Baking	1 kg potatoes (as wedges, unpeeled) 3 – 4 tbsp. rapeseed oil

(continued on next page)

Table S1: List of prepared dishes and the amounts of individual ingredients. (continued)

Dish	Preparation method	Ingredients
Brownies	Baking	Dough prepared from: 375 g butter 600 g dark chocolate 9 eggs 500 g sugar 16 g vanilla sugar 375 g flour 50 g cocoa 275 g walnuts (chopped)
Steaks	Grilling on gas grill	4 pork steaks, marinated (total 1100 — 1200 g) Marinade: rapeseed oil, onions, paprika
Vegetable skewers	Grilling on gas grill	10 vegetable skewers (total 1600 — 1800 g) made of zucchini, eggplant, bell pepper, mushroom, onion, garlic
Steaks	Grilling on charcoal grill	4 pork steaks, marinated (total 1050 — 1300 g) Marinade: rapeseed oil, onions, paprika

Table S2: MoLa instruments used for the measurements. For further information see Drewnick et al. (2012).

Instrument	Measured variable	Particle diameter range	Time resolution	Lower detection limit
CPC[a]	Particle number concentration	5 nm – 3 µm	1 s	N/A
FMPS[b]	Particle size distribution based on mobility diameter	5.6 – 560 nm	1 s	N/A
OPC[c]	Particle size distribution based on optical diameter	0.25 – 32 µm	6 s	N/A
Aethalometer[d]	Black and brown carbon mass concentrations	< 1.0 µm	1 s	< 5 ng m^{-3} (1-hour average)
MAAP[e]	Black carbon mass concentration	< 1.0 µm	60 s	0.01 µg m^{-3}
PAS[f]	Polyaromatic hydrocarbon mass concentration on particle surface	10 nm – 1 µm	12 s	1 ng m^{-3}
HR-ToF-AMS[g]	Size-dependent non-refractory chemical composition	40 nm – 1 µm	15 – 30 s	Sulfate: 0.04 µg m^{-3} Nitrate: 0.02 µg m^{-3} Ammonium: 0.05 µg m^{-3} Organics: 0.09 µg m^{-3} Chloride: 0.02 µg m^{-3}
AirPointer[h]	Mixing ratio of CO, SO_2, O_3	N/A	4 s	O_3: < 1.0 ppbv SO_2: < 1.0 ppbv CO: < 0.2 ppmv
NO_2/NO/NO_x Monitor[i]	Mixing ratio of NO_2, NO, NO_x	N/A	5 s	< 1 ppbv
LICOR[j]	Mixing ratio of CO_2	N/A	1 s	< 1 ppmv
Meteorological Station[k]	Wind speed, wind direction, relative humidity, temperature, rain intensity, pressure	N/A	1 s	N/A

[a]Condensation Particle Counter, model 3786, TSI, Inc., USA. [b]Fast Mobility Particle Sizer, model 3091, TSI, Inc., USA. [c]Optical Particle Counter, model 1.109, Grimm Aerosoltechnik, Germany. [d]Magee Scientific Aethalometer®, model AE33, Magee Scientific, USA; used for qualitative time series analysis only. [e]Multi-Angle Absorption Photometer, Carusso model 2012, Thermo Electron Corporation, USA. [f]Photoelectric Aerosol Sensor PAS2000, EcoChem Analytics, USA. [g]High-Resolution Time-of-Flight Aerosol Mass Spectrometer, Aerodyne Research, Inc., USA. [h]AirPointer, Recordum Messtechnik GmbH, Austria. [i]NO2/NO/NO_x Monitor, model 405 nm, 2B Technologies, Inc., USA. [j]LI840, LI-COR, Inc., USA. [k]WXT520, Vaisala, Finland.

Table S3: List of mass spectra used as reference to calculate average mass spectra for the respective aerosol types (Ulbrich et al., 2023).

Spectrum ID	Aerosol type	Reference
A_HR_001	HOA	Docherty et al. (2011)
A_HR_003	LVOOA	Docherty et al. (2011)
A_HR_004	SVOOA	Docherty et al. (2011)
A_HR_005	BBOA	Aiken et al. (2009)
A_HR_006	HOA	Aiken et al. (2009)
A_HR_007	LVOOA	Aiken et al. (2009)
A_HR_008	SVOOA	Aiken et al. (2009)
A_HR_013	BBOA	Mohr et al. (2012)
A_HR_014	COA	Mohr et al. (2012)
A_HR_015	HOA	Mohr et al. (2012)
A_HR_016	LVOOA	Mohr et al. (2012)
A_HR_017	SVOOA	Mohr et al. (2012)
A_HR_018	HOA	Setyan et al. (2012)
A_HR_019	LOOOA	Setyan et al. (2012)
A_HR_020	MOOOA	Setyan et al. (2012)
A_HR_021	OOAa	Saarikoski et al. (2012)
A_HR_022	OOAb	Saarikoski et al. (2012)
A_HR_023	OOAc	Saarikoski et al. (2012)
A_HR_024	HOA	Saarikoski et al. (2012)
A_HR_025	BBOA	Saarikoski et al. (2012)
A_HR_026	NOA	Saarikoski et al. (2012)
A_HR_027	COA	Crippa et al. (2013b)
A_HR_028	SVOOA	Crippa et al. (2013b)
A_HR_030	LV-OOA	Crippa et al. (2013b)
A_HR_031	HOA	Crippa et al. (2013b)
A_HR_032	BBOA	Elser et al. (2016)
A_HR_033	HOA	Elser et al. (2016)
A_HR_034	COA	Elser et al. (2016)
A_HR_035	CCOA	Elser et al. (2016)
A_HR_036	OOA	Elser et al. (2016)

(continued on next page)

Table S3: List of mass spectra used as reference to calculate average mass spectra for the respective aerosol types (Ulbrich et al., 2023). (continued)

Spectrum ID	Aerosol type	Reference
A_HR_037	BBOA	Struckmeier et al. (2016)
A_HR_038	COA	Struckmeier et al. (2016)
A_HR_039	HOA	Struckmeier et al. (2016)
A_HR_040	LVOOA	Struckmeier et al. (2016)
A_HR_041	SVOOA	Struckmeier et al. (2016)
A_HR_042	COA	Struckmeier et al. (2016)
A_HR_043	HOA	Struckmeier et al. (2016)
A_HR_044	LVOOA	Struckmeier et al. (2016)
A_HR_045	SVOOA	Struckmeier et al. (2016)
A_HR_046	CSOA	Struckmeier et al. (2016)
A_HR_047	HOA	Hayes et al. (2013)
A_HR_048	COA	Hayes et al. (2013)
A_HR_050	LVOOA	Hayes et al. (2013)
A_HR_051	SVOOA	Hayes et al. (2013)
A_HR_055	CCOA	Hu et al. (2013)
A_HR_056	HOA	Hu et al. (2013)
A_HR_057	SVOOA	Hu et al. (2013)
A_HR_058	LVOOA	Hu et al. (2013)
A_HR_059	HOA	Hu et al. (2016)
A_HR_060	COA	Hu et al. (2016)
A_HR_061	LOOOA	Hu et al. (2016)
A_HR_062	MOOOA	Hu et al. (2016)
A_HR_063	LOOOA	Hu et al. (2016)
A_HR_064	MOOOA	Hu et al. (2016)
A_HR_065	COA	Hu et al. (2016)
A_HR_066	HOA	Hu et al. (2016)
A_HR_067	BBOA	Hu et al. (2016)
A_HR_068	CCOA	Hu et al. (2016)
A_HR_069	IEPOX-SOA	Hu et al. (2015)
A_HR_070	MOOOA	Hu et al. (2015)

(continued on next page)

Table S3: List of mass spectra used as reference to calculate average mass spectra for the respective aerosol types (Ulbrich et al., 2023). (continued)

Spectrum ID	Aerosol type	Reference
A_HR_071	LOOOAI	Hu et al. (2015)
A_HR_072	LOOOAII	Hu et al. (2015)
A_HR_073	MOOOA	Hu et al. (2018)
A_HR_074	LOOOA	Hu et al. (2018)
A_HR_075	HOA	Hu et al. (2018)
A_DEC_C_032	HOA	Hersey et al. (2011)
A_DEC_C_033	LVOOA	Hersey et al. (2011)
A_DEC_C_034	SVOOA	Hersey et al. (2011)
A_DEC_W_035	BBOA	Crippa et al. (2013a)
A_DEC_W_036	COA	Crippa et al. (2013a)
A_DEC_W_037	HOA	Crippa et al. (2013a)
A_DEC_W_038	LVOOA	Crippa et al. (2013a)
A_DEC_C_044	HOA	Craven et al. (2013)
A_DEC_C_045	SVOOA	Craven et al. (2013)
A_DEC_C_046	LVOOA	Craven et al. (2013)

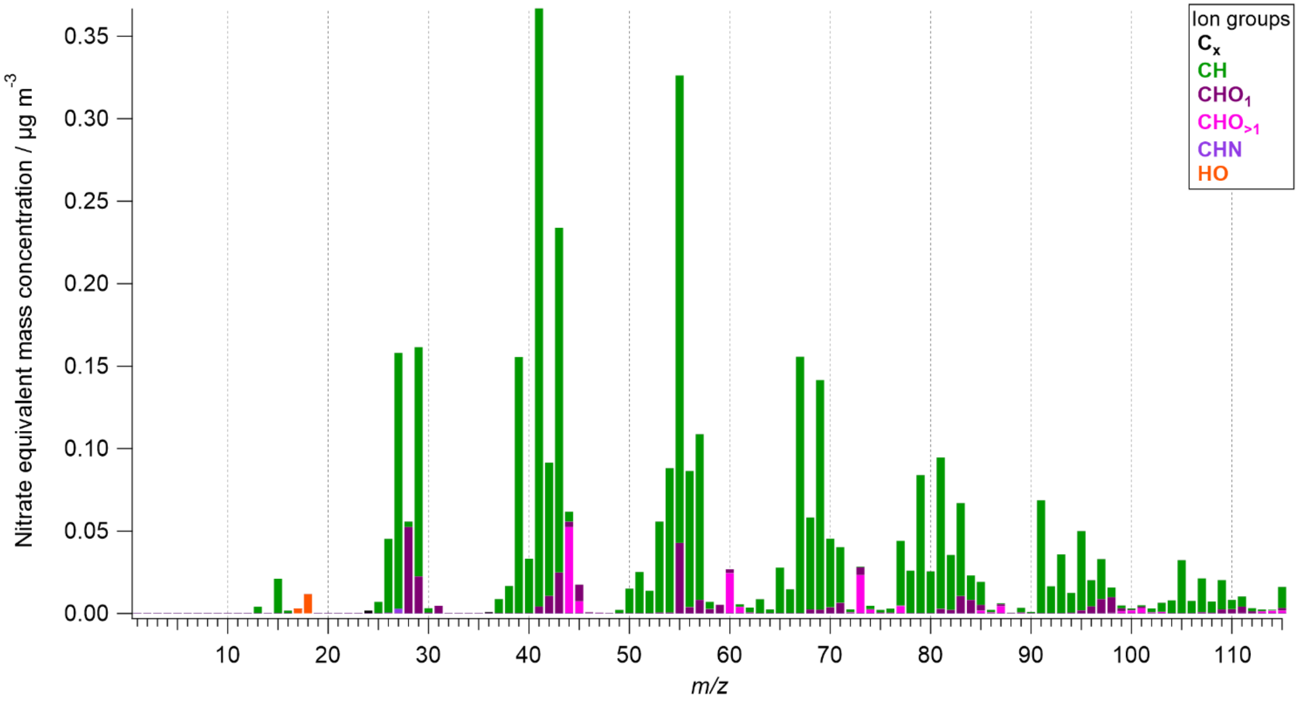

Figure S1: Organic mass spectrum of heated rapeseed oil measured with the HR-ToF-AMS.

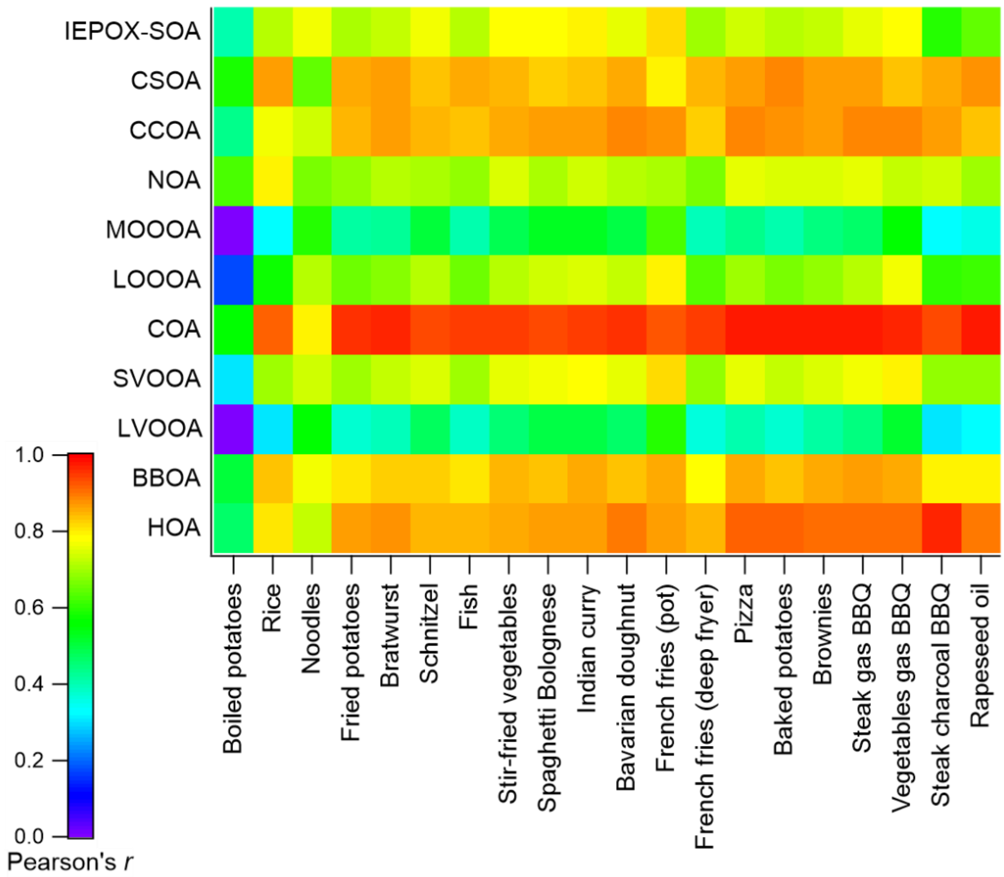

95 **Figure S2: Linear correlation of the averaged organic mass spectra of cooking emissions for all laboratory experiments and pure rapeseed oil with average mass spectra of different aerosol types from the AMS spectra database (Ulbrich et al., 2023), color-coded based on the respective correlation coefficient (Pearson's *r*). The list of the used mass spectra is in Table S3.**

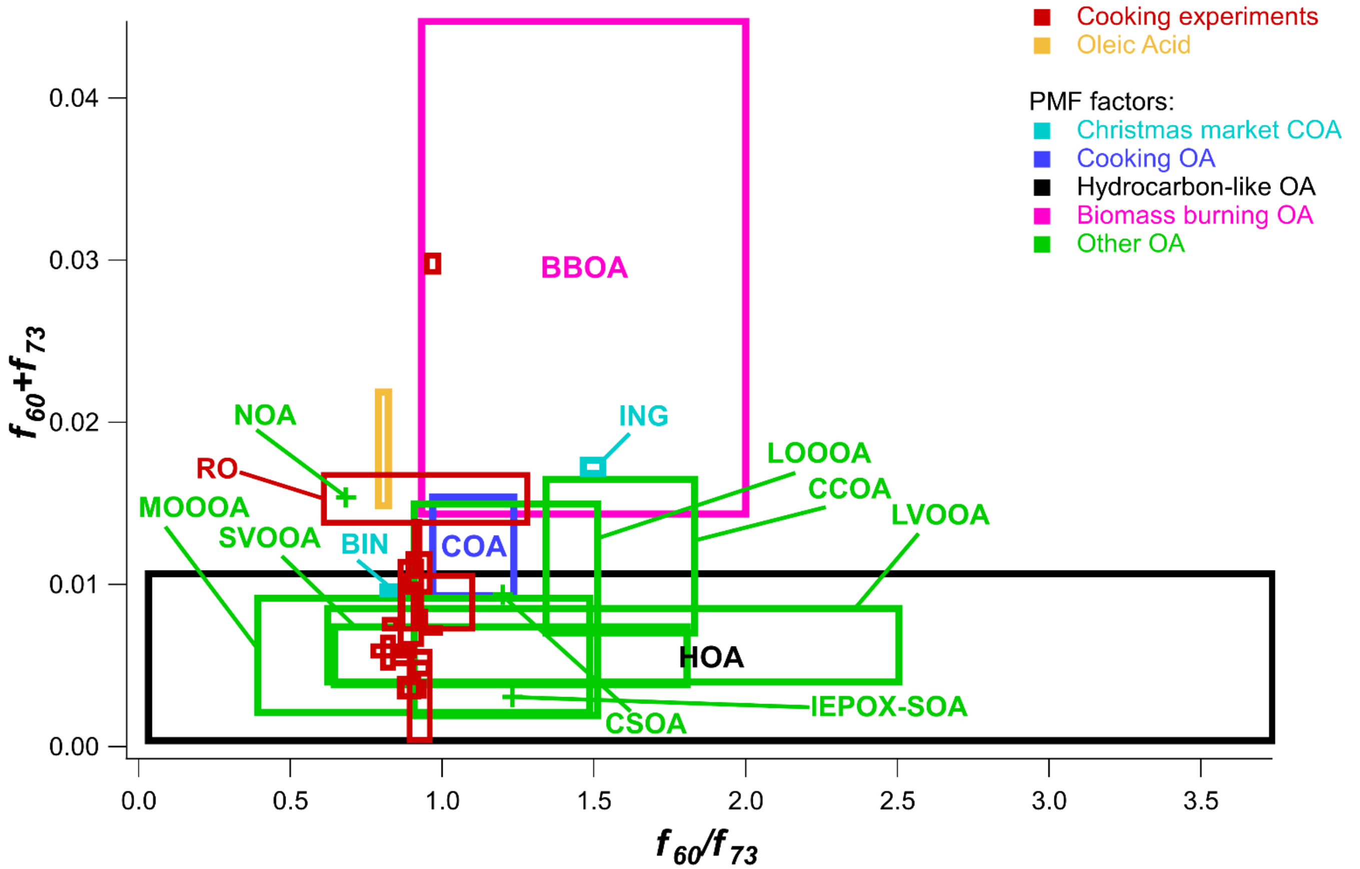

Figure S3: "Rectangle plot" of f60+f73 combined with f60/f73 for the cooking experiments, the Christmas markets, and various organic aerosol types from ambient measurements. The rectangles represent one standard deviation of the markers for the respective aerosol types as found in mass spectra from the literature. The acronyms for the different aerosol types are listed in Table 2; RO stands for rapeseed oil. The cooking experiment related outlier in the BBOA box is from the brownies experiment, possibly related to charring of material on the oven walls.

Table S4: Average ratio of signal intensities at *m/z* 67 and 69 from mass spectra of different aerosol types. The standard deviation was calculated from the available data using the AMS spectra database (Ulbrich et al., 2023). If no standard deviation is stated, only a single mass spectrum was available for the respective aerosol type.

Aerosol type	Ratio of signal intensities at *m/z* 67 and 69
HOA	0.63 ± 0.30
BBOA	0.63 ± 0.36
LVOOA	0.78 ± 0.43
SVOOA	0.88 ± 0.53
LOOOA	0.87 ± 0.50
MOOOA	1.03 ± 0.80
NOA	0.55
CCOA	0.61 ± 0.15
CSOA	0.72
IEPOX-SOA	0.71

Table S5: RIE_{COA} and density values derived from the presented laboratory experiments and other studies.

Dishes / measurements	RIE_{COA}	Density / g cm^{-3}
Laboratory experiments		
Fried potatoes	2.03	0.96
Bratwurst	2.17	0.94
Schnitzel	2.34	0.99
Fish	2.48	0.96
Spaghetti Bolognese	1.53	1.03
Indian curry	2.16	1.01
Stir-fried vegetables	1.83	1.01
Bavarian doughnut	1.83	1.03
French fries (pot)	1.58	0.96
French fries (deep fryer)	2.52	0.97
Steak gas BBQ (grilling)	2.11	0.98
Vegetables gas BBQ (grilling)	1.79	0.97
Steak charcoal BBQ (grilling)	2.27	0.91
Steak gas BBQ (warm up)[a]	1.53	0.98
Vegetables gas BBQ (warm up)[a]	1.79	0.97
Steak charcoal BBQ (warm up)[a]	2.51	0.91
Average ± standard deviation	2.05 ± 0.32	0.98 ± 0.03
Reyes-Villegas et al. (2018) – values for diluted emission measurements		
Deep fried plus English breakfast	2.63	
English breakfast	2.35	
Deep fried	3.06	
Shallow fried meat (stir fried)	1.85	
Shallow fried meat (chops)	1.56	
Average ± standard deviation	2.29 ± 0.60	

[a]Value not included in average RIE_{COA} and density.

(continued on next page)

Table S5: RIECOA and density values derived from the presented laboratory experiments and other studies. (continued)

Dishes / measurements	**RIE_{COA}**	**Density / g cm^{-3}**
Katz et al. (2021)		
ATHLETIC Nov. 6	4.61 ± 1.52	0.95
ATHLETIC Nov. 7	4.96 ± 1.64	
ATHLETIC Nov. 16	4.26 ± 1.41	
HOMEChem Thanksgiving	5.73 ± 1.89	1.0
HOMEChem Breakfast	6.50 ± 2.15	
HOMEChem Stir Fry	4.70 ± 1.55	
HOMEChem Beef Chili	5.35 ± 1.77	
Average ± standard deviation	5.16 ± 0.77	

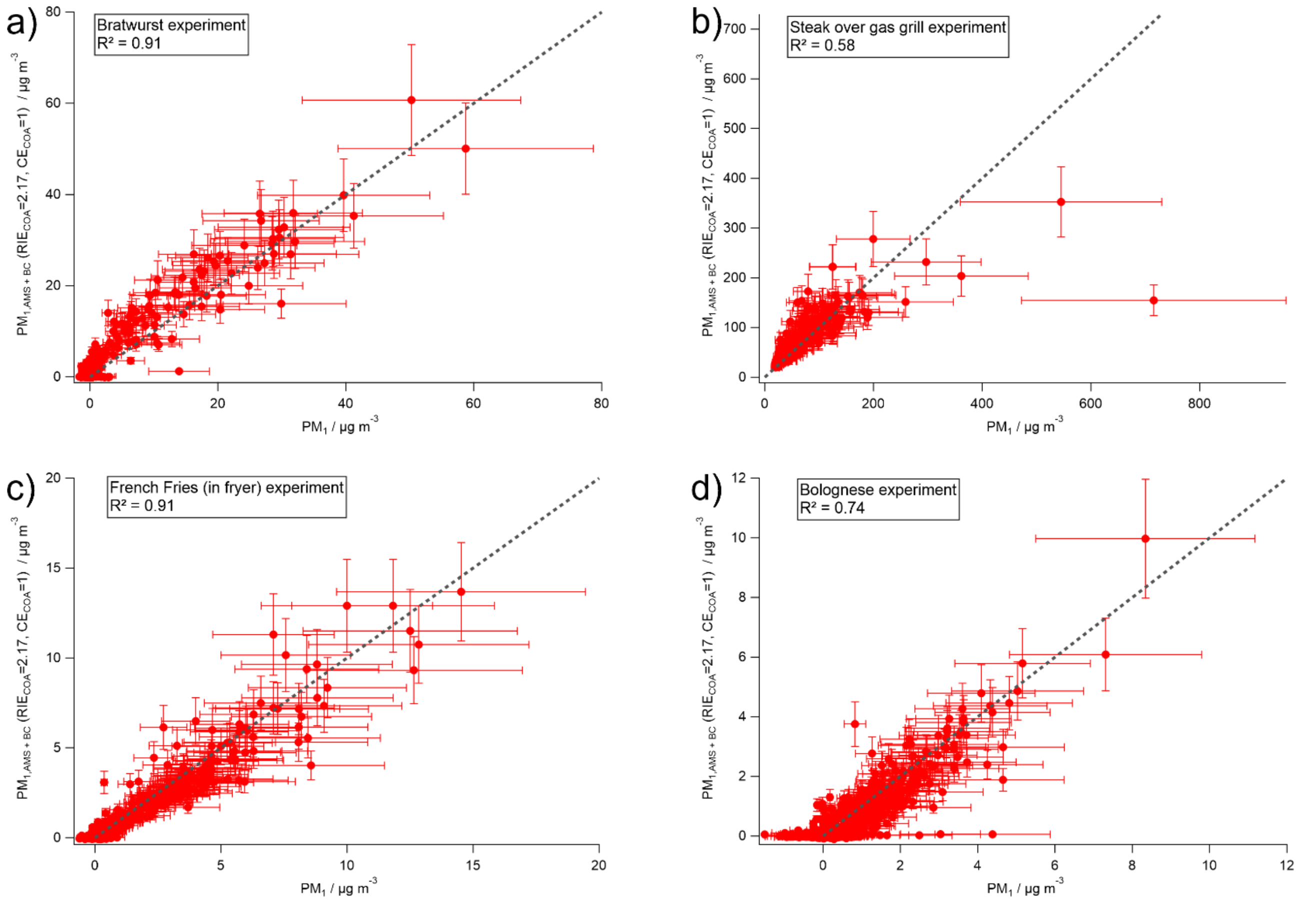

Figure S4: Typical example correlations (using ODR-fitting) between PM_1 calculated from AMS and BC data and PM_1 calculated from size distribution data. The AMS RIE values have been adjusted to give a slope of 1.0 in the correlations and are shown on the y-axis labels. Pearson's R^2 values are shown in the boxes.

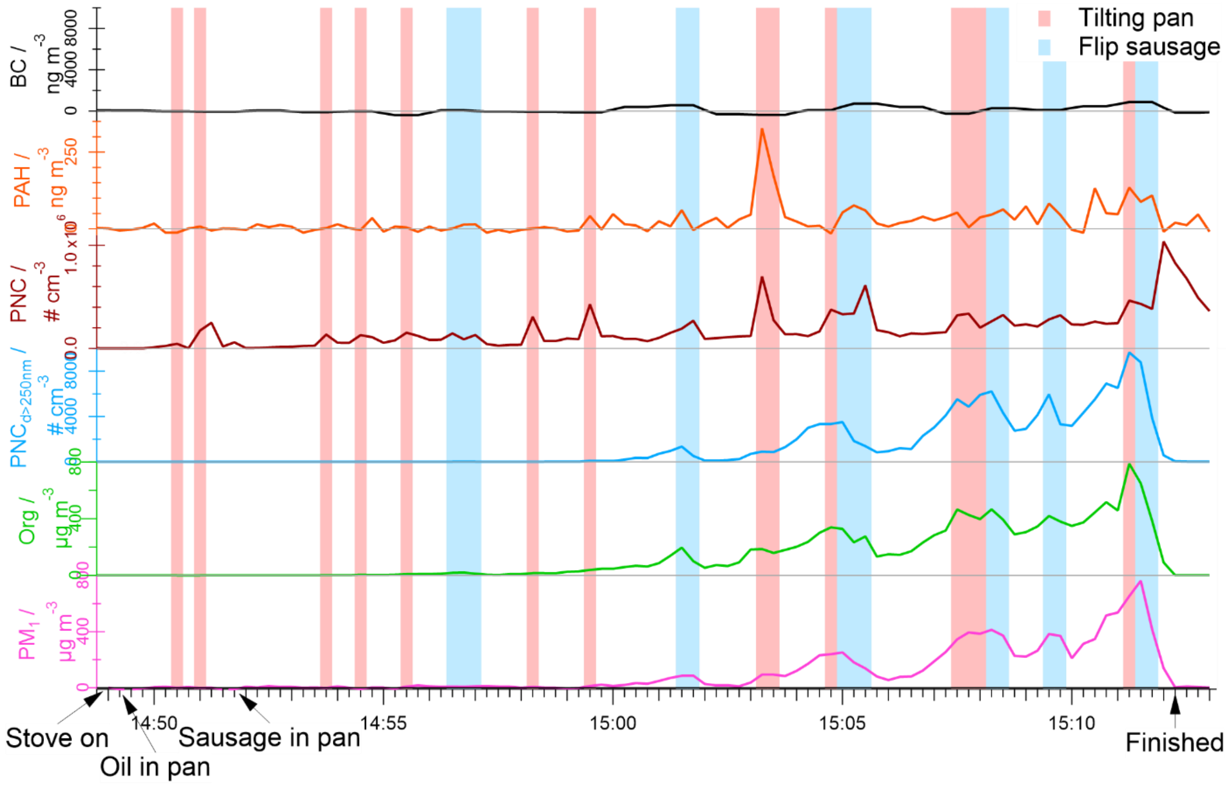

130 **Figure S5: Time series of the six most relevant variables for the experiment "frying bratwurst". Highlighted in red and blue are the activities "tilting pan" and "flip sausage" during the experiment.**

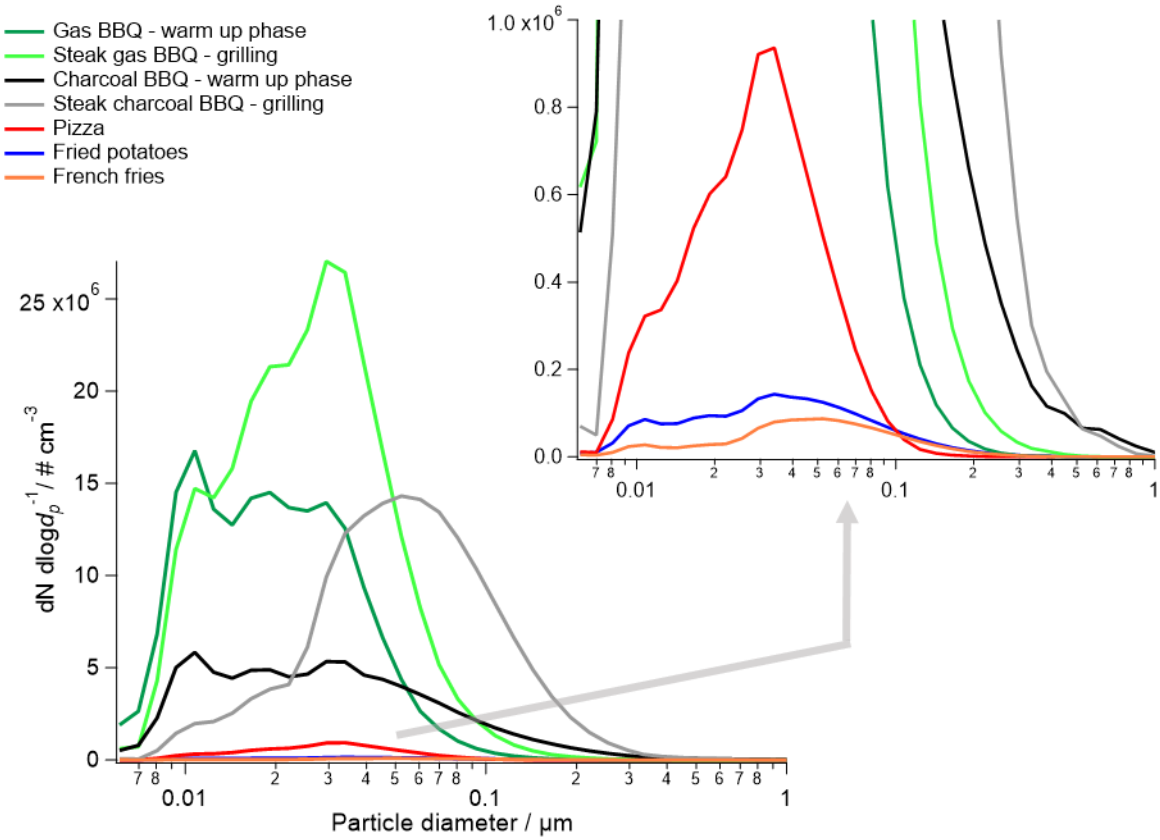

Figure S6: Averaged particle number size distribution for five dishes, one exemplary dish for each preparation method (except boiling due to low concentrations). For the grilling experiments, the warm up and grilling period were averaged separately. The upper right insert is a magnified close-up of the size distributions.

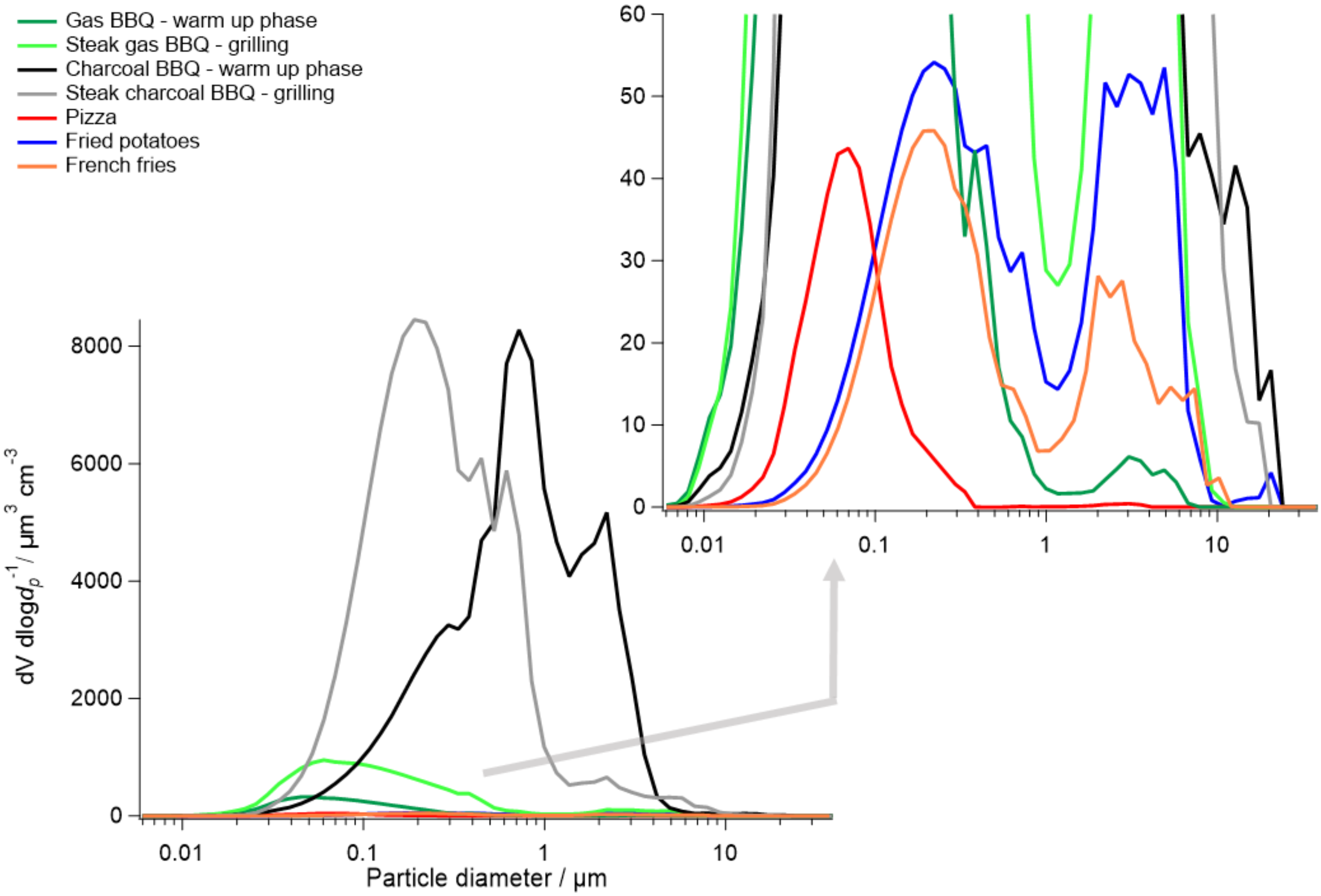

140 **Figure S7: Averaged particle volume size distribution for five dishes, one exemplary dish for each preparation method (except boiling due to low concentrations). For the grilling experiments, the warm up and grilling period were averaged separately. The upper right insert is a magnified close-up of the size distributions.**

Table S6: Emission factors (average and standard deviation) for the measured variables and all dishes. No values are listed if the calculated values were negative or if there was no increase of the concentration compared to background.

Dishes	**PN / kg^{-1}**		**PM_1 / g kg^{-1}**		**$PM_{2.5}$ / g kg^{-1}**		**PM_{10} / g kg^{-1}**		**Organics / mg kg^{-1}**		**$PN_{d>250\ nm}$ / kg^{-1}**	
	AVG	STD	AVG	STD	AVG	STD	AVG	STD	AVG	STD	AVG	STD
Boiled potatoes	$3\cdot10^{12}$	$4.7\cdot10^{12}$	$1.7\cdot10^{-4}$	$1.4\cdot10^{-4}$	$1.9\cdot10^{-4}$	$1.4\cdot10\text{-}^{4}$	$2.7\cdot10^{-4}$	$2.1\cdot10^{-4}$	0.05	0.05	$5\cdot10^{7}$	$2\cdot10^{8}$
Rice	$1.8\cdot10^{12}$	$1.6\cdot10^{12}$	$1.0\cdot10^{-3}$	$5.1\cdot10^{-4}$	$1.0\cdot10^{-3}$	$5.2\cdot10^{-4}$	$1.0\cdot10^{-3}$	$5.2\cdot10^{-4}$	0.34	0.36	$9.3\cdot10^{9}$	$5.4\cdot10^{9}$
Noodles	$1.4\cdot10^{12}$	$3.1\cdot10^{11}$	$1.3\cdot10^{-3}$	$1.2\cdot10^{-4}$	$1.3\cdot10^{-3}$	$3.2\cdot10^{-5}$	$1.3\cdot10^{-3}$	$4.9\cdot10^{-5}$	0.19	0.0067	$9\cdot10^{9}$	$4\cdot10^{9}$
Fried potatoes	$4\cdot10^{13}$	$9.2\cdot10^{12}$	$1.7\cdot10^{-2}$	$6.3\cdot10^{-3}$	$2.0\cdot10^{-2}$	$6.7\cdot10^{-3}$	$2.8\cdot10^{-2}$	$7.2\cdot10^{-3}$	14	5.8	$2\cdot10^{11}$	$5\cdot10^{10}$
Bratwurst	$4.8\cdot10^{13}$	$1.1\cdot10^{13}$	$1.8\cdot10^{-2}$	$7.4\cdot10^{-3}$	$1.8\cdot10^{-2}$	$1.2\cdot10^{-2}$	$1.9\cdot10^{-2}$	$1.2\cdot10^{-2}$	23	10	$2\cdot10^{11}$	$1\cdot10^{11}$
Schnitzel	$1.9\cdot10^{13}$	$3.3\cdot10^{12}$	$3.9\cdot10^{-3}$	$2.3\cdot10^{-4}$	$5.0\cdot10^{-3}$	$5.9\cdot10^{-4}$	$5.7\cdot10^{-3}$	$7.2\cdot10^{-4}$	3.3	0.087	$3\cdot10^{10}$	$3\cdot10^{9}$
Fish	$4.6\cdot10^{13}$	$7.3\cdot10^{12}$	$2.6\cdot10^{-2}$	$6.5\cdot10^{-3}$	$3.0\cdot10^{-2}$	$9.8\cdot10^{-3}$	$3.4\cdot10^{-2}$	$8.9\cdot10^{-3}$	27	7.9	$3\cdot10^{11}$	$1\cdot10^{11}$
Spaghetti Bolognese	$7.6\cdot10^{12}$	$3.1\cdot10^{12}$	$2.4\cdot10^{-3}$	$3.3\cdot10^{-4}$	$3.2\cdot10^{-3}$	$1.7\cdot10^{-4}$	$4.0\cdot10^{-3}$	$1.0\cdot10^{-4}$	1.9	0.24	$3\cdot10^{10}$	$2\cdot10^{9}$
Indian curry	$6.2\cdot10^{12}$	$3.6\cdot10^{12}$	$1.3\cdot10^{-3}$	$2.8\cdot10^{-4}$	$2.0\cdot10^{-3}$	$2.4\cdot10^{-4}$	$2.5\cdot10^{-3}$	$3.3\cdot10^{-4}$	1	0.3	$2\cdot10^{10}$	$5\cdot10^{9}$
Stir-fried vegetables	$7.8\cdot10^{12}$	$3\cdot10^{12}$	$2.2\cdot10^{-3}$	$1.1\cdot10^{-3}$	$3.1\cdot10^{-3}$	$6.5\cdot10^{-4}$	$3.9\cdot10^{-3}$	$6.8\cdot10^{-4}$	2.2	0.64	$2\cdot10^{10}$	$7\cdot10^{9}$
Bavarian doughnut	$5.5\cdot10^{12}$	$5.8\cdot10^{11}$	$5.5\cdot10^{-3}$	$3.2\cdot10^{-3}$	$5.6\cdot10^{-3}$	$5.3\cdot10^{-3}$	$5.7\cdot10^{-3}$	$5.3\cdot10^{-3}$	4.9	4.3	$5\cdot10^{10}$	$5\cdot10^{10}$
French fries (pot)	$1.1\cdot10^{13}$	$6.5\cdot10^{12}$	$3.8\cdot10^{-3}$	$1.9\cdot10^{-3}$	$5.0\cdot10^{-3}$	$2.3\cdot10^{-3}$	$5.8\cdot10^{-3}$	$2.5\cdot10^{-3}$	3.2	2	$4\cdot10^{10}$	$3\cdot10^{10}$
French fries (deep fryer)	$1.1\cdot10^{13}$	$5.6\cdot10^{12}$	$6.3\cdot10^{-3}$	$8.4\cdot10^{-4}$	$7.5\cdot10^{-3}$	$1.0\cdot10^{-3}$	$9.1\cdot10^{-3}$	$1.2\cdot10^{-3}$	5.6	1.1	$1\cdot10^{11}$	$2\cdot10^{10}$
Pizza	$1.3\cdot10^{14}$	$4.2\cdot10^{13}$	$7.0\cdot10^{-3}$	$2.5\cdot10^{-3}$	$7.0\cdot10^{-3}$	$2.6\cdot10^{-3}$	$7.1\cdot10^{-3}$	$2.6\cdot10^{-3}$	5.5	2	$8\cdot10^{7}$	$5\cdot10^{7}$
Baked potatoes	$3.3\cdot10^{13}$	$7.7\cdot10^{12}$	$6.9\cdot10^{-4}$	$1.5\cdot10^{-4}$	$7.4\cdot10^{-4}$	$1.3\cdot10^{-4}$	$7.7\cdot10^{-4}$	$1.5\cdot10^{-4}$	0.53	0.19		
Brownies	$2.1\cdot10^{12}$	$1.3\cdot10^{12}$	$1.6\cdot10^{-3}$	$1.0\cdot10^{-4}$	$1.6\cdot10^{-3}$	$3.1\cdot10^{-5}$	$1.6\cdot10^{-3}$	$3.8\cdot10^{-5}$	1.2	0.4	$2\cdot10^{10}$	$3\cdot10^{9}$
Steak gas BBQ	$3.9\cdot10^{15}$	$1\cdot10^{15}$	0.17	0.049	0.17	0.044	0.18	0.046	180	33	$7\cdot10^{11}$	$6\cdot10^{10}$
Vegetables gas BBQ	$3\cdot10^{15}$	$1.7\cdot10^{14}$	0.23	0.11	0.23	0.077	0.24	0.078	260	66	$9\cdot10^{11}$	$3\cdot10^{11}$
Steak charcoal BBQ	$2.7\cdot10^{15}$	$2.3\cdot10^{14}$	2.4	0.32	2.4	0.48	2.4	0.49	2100	350	$2\cdot10^{13}$	$3\cdot10^{12}$

(continued on next page)

Table S6: Emission factors (average and standard deviation) for the measured variables and all dishes. No values are listed if the calculated values were negative or if there was no increase of the concentration compared to background. (continued)

Dishes	BC / µg kg^{-1}		PAH / µg kg^{-1}		Sulfate / µg kg^{-1}		Chloride / µg kg^{-1}		Ammonium/ µg kg^{-1}		Nitrate / µg kg^{-1}		NO_x[a] / mg kg^{-1}	
	AVG	STD	AVG	STD	AVG	STD	AVG	STD	AVG	STD	AVG	STD	AVG	STD
Boiled potatoes														
Rice														
Noodles														
Fried potatoes	220	83	27	7.7			13	4						
Bratwurst	18	6	4.2	2.1			35	14	9	2				
Schnitzel							31	5	2	0.4				
Fish	380	100	3.4	1.5			59	6	12	2	38	18		
Spaghetti Bolognese					15	16								
Indian curry					6	7								
Stir-fried vegetables					52	23			2	2				
Bavarian doughnut														
French fries (pot)									1	1				
French fries (deep fryer)	57	16							3	1				
Pizza	23	9												
Baked potatoes														
Brownies														
Steak gas BBQ	490	22	13	2.5	26	14	400	116	59	16	914	262	190	18
Vegetables gas BBQ	490	350	16	3.6	36	6	259	136	72	19	381	227	141	12
Steak charcoal BBQ	28000	13000	208	99	354	18	1953	528	311	56	1071	175	337	50

[a]Conversion from volume mixing ratio to mass concentration assuming NO_x is fully converted to NO_2.

Table S7: Criteria to calculate emissions from different emission sources for comparison with cooking emissions and references for the used emissions factors.

Source	**Activity**	**References of the used emission factors**
Cooking	Cooking the dish once	This work
Driving a car	Driving over 100 km	Alves et al., 2015; Conte and Contini, 2019; Ho et al., 2009; Imhof et al., 2005; Imhof et al., 2006; Jones and Harrison, 2006; Kittelson et al., 2004; Kostenidou et al., 2021; Wang et al., 2009; Zheng et al., 2018
Wood home heating	Heating a room of 50 m^2 for 1 h (calorific requirement 60 kWh m^{-2} a^{-1})	Bäfver et al., 2011; Boman et al., 2011; Fachinger et al., 2017; Johansson et al., 2004; Shen et al., 2012
Candle burning	Burning candle for 1 h	Andersen et al., 2021; Derudi et al., 2014; Pagels et al., 2009; Stabile et al., 2012; Zai et al., 2006
Cigarette smoking	Smoking 2 cigarettes	Daher et al., 2010; Endo et al., 2000; Hearn et al., 2018; Ruprecht et al., 2017; Savdie et al., 2020; Wallace and Ott, 2011

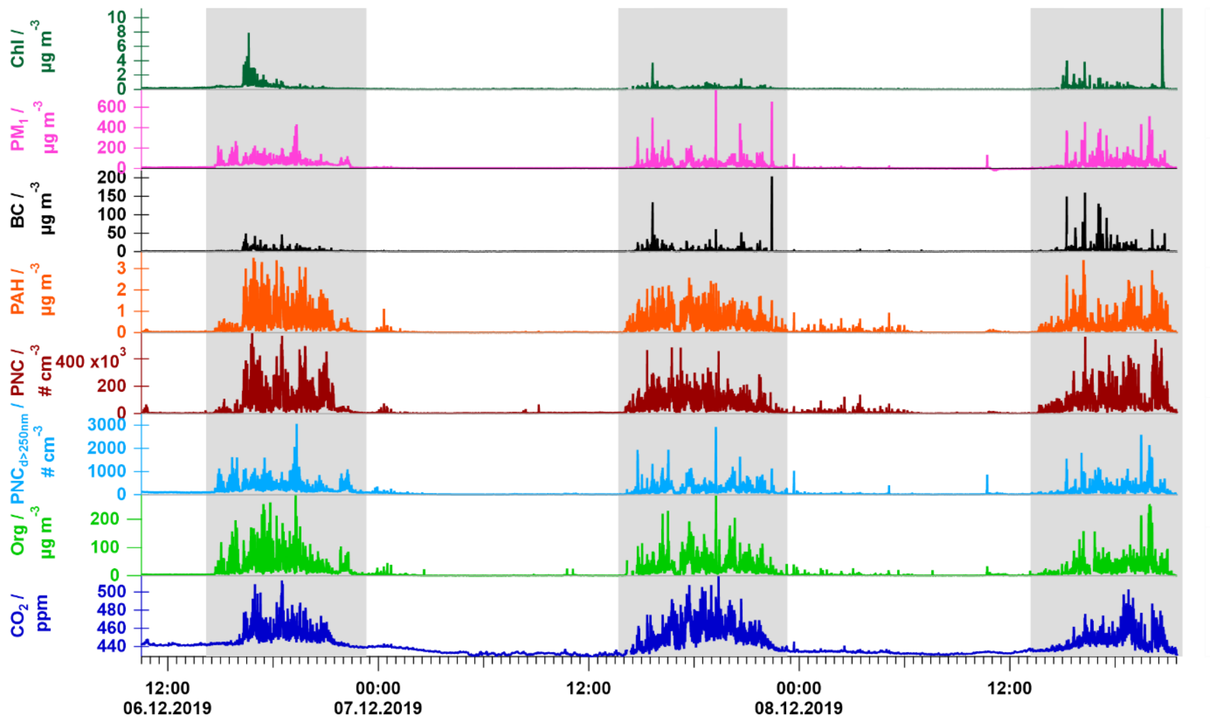

155

Figure S8: Time series of variables for which the concentrations increased during the Christmas market opening hours (gray shading) in Ingelheim.

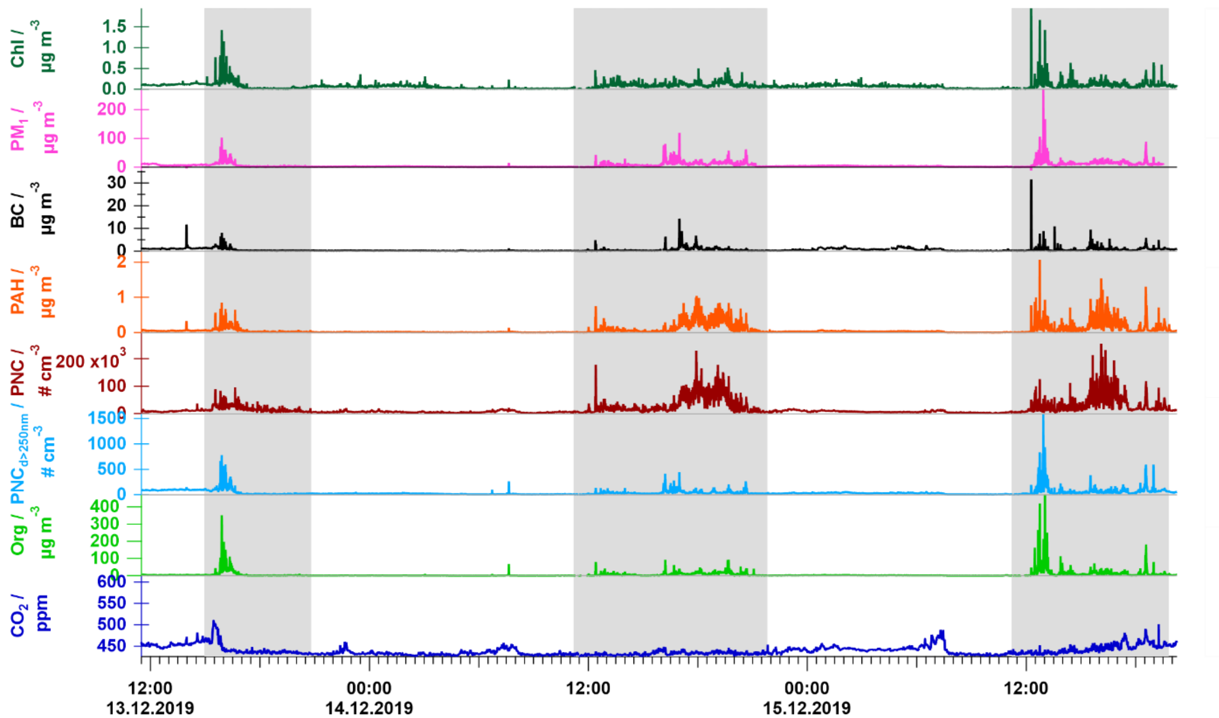

Figure S9: Time series of variables for which the concentrations increased during the Christmas market opening hours (gray shading) in Bingen.

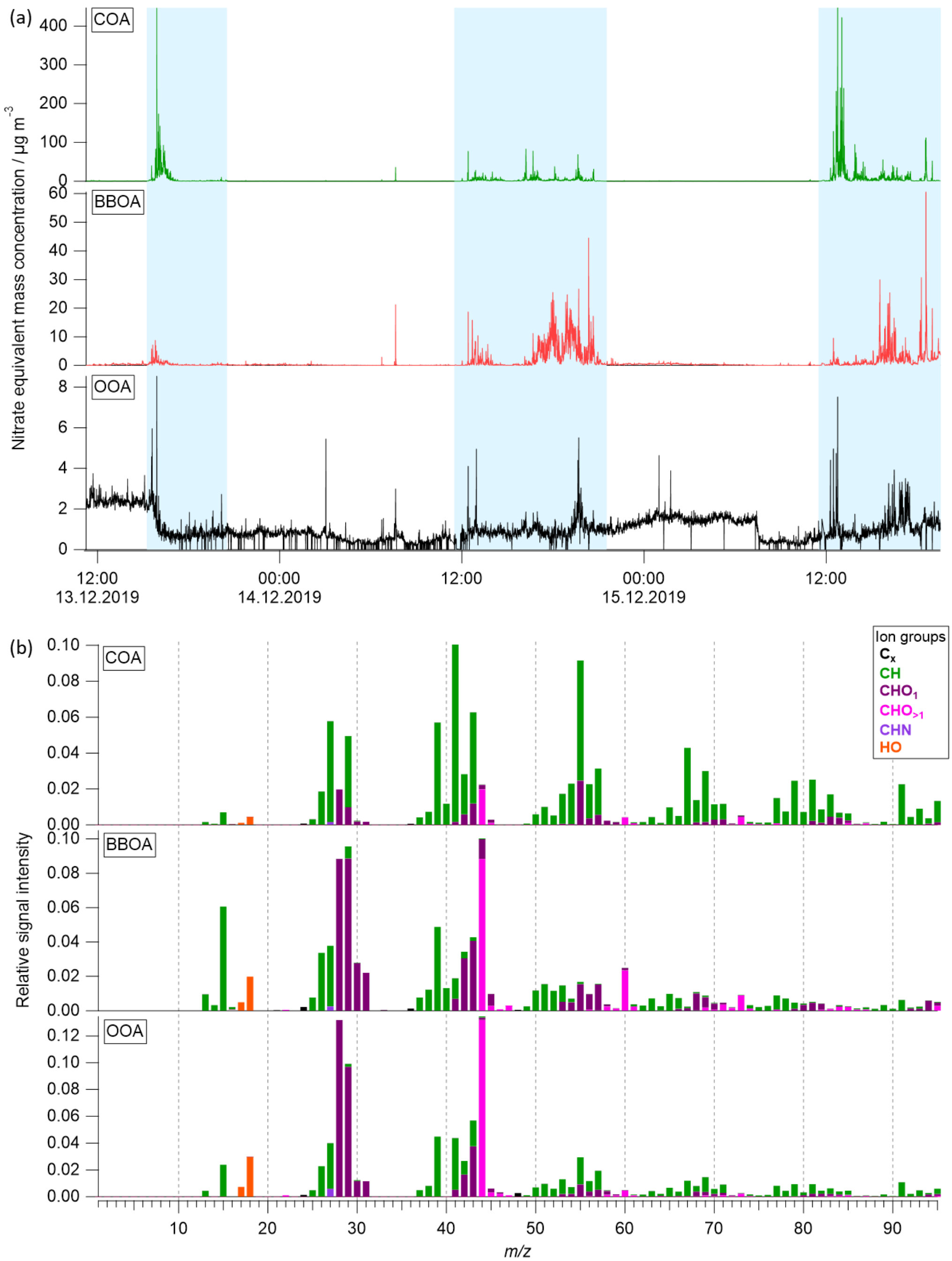

Figure S10: Time series (a) and mass spectra (b) of the chosen PMF-solution representing the aerosol types COA, BBOA, and OOA during the measurements at the Christmas market in Bingen. The opening hours are highlighted in blue.

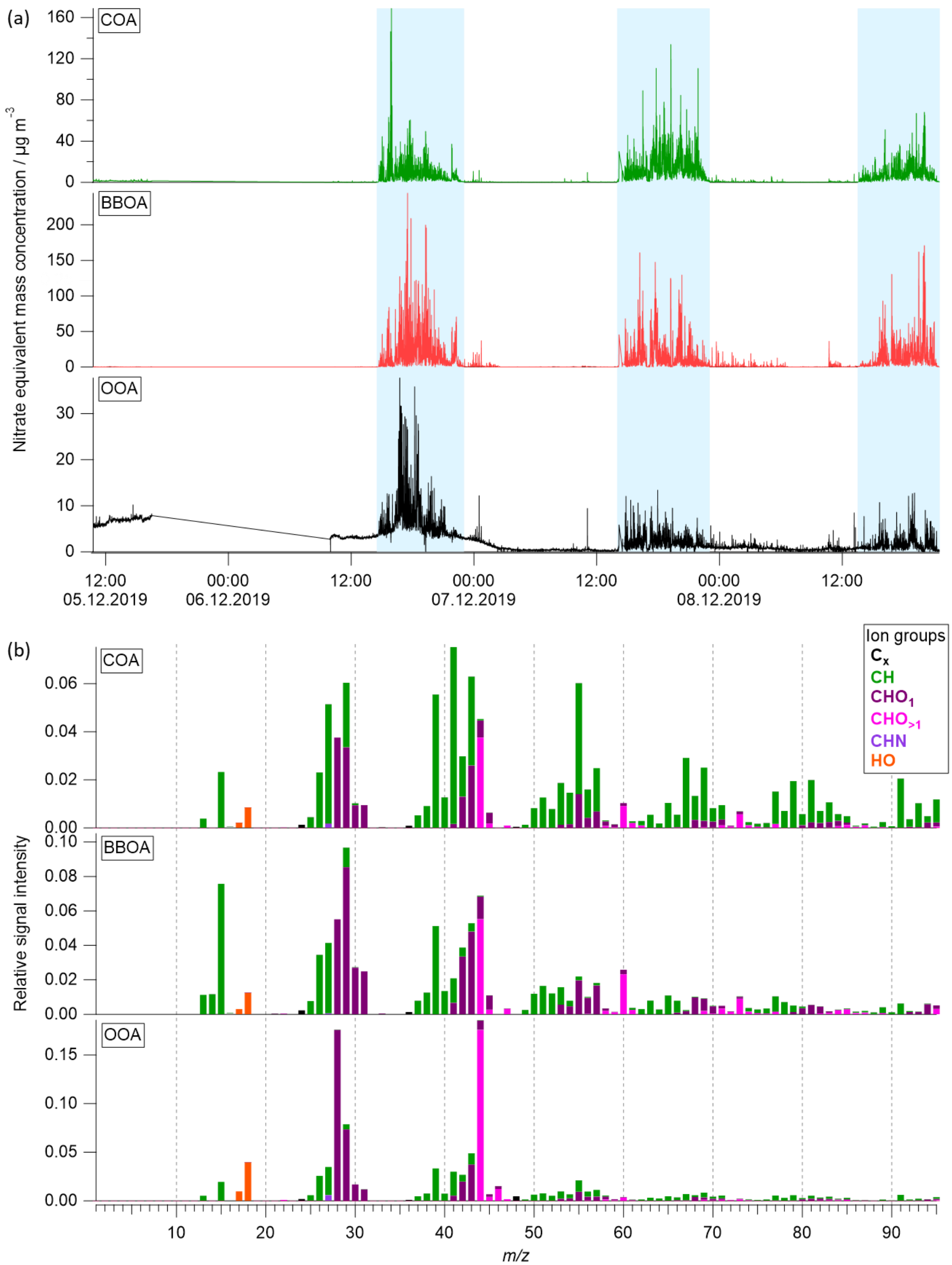

Figure S11: Time series (a) and mass spectra (b) of the chosen PMF-solution representing the aerosol types COA, BBOA, and OOA during the measurements at the Christmas market in Ingelheim. The opening hours are highlighted in blue.

References

Aiken, A. C., Salcedo, D., Cubison, M. J., Huffman, J. A., DeCarlo, P. F., Ulbrich, I. M., Docherty, K. S., Sueper, D., Kimmel, J. R., Worsnop, D. R., Trimborn, A., Northway, M., Stone, E. A., Schauer, J. J., Volkamer, R. M., Fortner, E., Foy, B. de, Wang, J., Laskin, A., Shutthanandan, V., Zheng, J., Zhang, R., Gaffney, J., Marley, N. A., Paredes-Miranda, G., Arnott, W. P., Molina, L. T., Sosa, G., and Jimenez, J. L.: Mexico City aerosol analysis during MILAGRO using high resolution aerosol mass spectrometry at the urban supersite (T0) – Part 1: Fine particle composition and organic source apportionment, Atmos. Chem. Phys., 9, 6633–6653, https://doi.org/10.5194/acp-9-6633-2009, 2009.

Andersen, C., Omelekhina, Y., Rasmussen, B. B., Nygaard Bennekov, M., Skov, S. N., Køcks, M., Wang, K., Strandberg, B., Mattsson, F., Bilde, M., Glasius, M., Pagels, J., and Wierzbicka, A.: Emissions of soot, PAHs, ultrafine particles, NOx, and other health relevant compounds from stressed burning of candles in indoor air, Indoor Air, 31, 2033–2048, https://doi.org/10.1111/ina.12909, 2021.

Bäfver, L. S., Leckner, B., Tullin, C., and Berntsen, M.: Particle emissions from pellets stoves and modern and old-type wood stoves, Biomass and Bioenergy, 35, 3648–3655, https://doi.org/10.1016/j.biombioe.2011.05.027, 2011.

Baron, P. A., Kulkarni, P., and Willeke, K. (Eds.): Aerosol measurement: Principles, techniques, and applications, 3rd ed., Engineering professional collection, John Wiley & Sons, Inc., New York, 883 pp., 2011.

Boman, C., Pettersson, E., Westerholm, R., Boström, D., and Nordin, A.: Stove Performance and Emission Characteristics in Residential Wood Log and Pellet Combustion, Part 1: Pellet Stoves, Energy Fuels, 25, 307–314, https://doi.org/10.1021/ef100774x, 2011.

Craven, J. S., Metcalf, A. R., Bahreini, R., Middlebrook, A., Hayes, P. L., Duong, H. T., Sorooshian, A., Jimenez, J. L., Flagan, R. C., and Seinfeld, J. H.: Los Angeles Basin airborne organic aerosol characterization during CalNex, J. Geophys. Res. Atmos., 118, 11,453-11,467, https://doi.org/10.1002/jgrd.50853, 2013.

Crippa, M., DeCarlo, P. F., Slowik, J. G., Mohr, C., Heringa, M. F., Chirico, R., Poulain, L., Freutel, F., Sciare, J., Cozic, J., Di Marco, C. F., Elsasser, M., Nicolas, J. B., Marchand, N., Abidi, E., Wiedensohler, A., Drewnick, F., Schneider, J., Borrmann, S., Nemitz, E., Zimmermann, R., Jaffrezo, J.-L., Prévôt, A. S. H., and Baltensperger, U.: Wintertime aerosol chemical composition and source apportionment of the organic fraction in the metropolitan area of Paris, Atmos. Chem. Phys., 13, 961–981, https://doi.org/10.5194/acp-13-961-2013, 2013a.

Crippa, M., El Haddad, I., Slowik, J. G., DeCarlo, P. F., Mohr, C., Heringa, M. F., Chirico, R., Marchand, N., Sciare, J., Baltensperger, U., and Prévôt, A. S. H.: Identification of marine and continental aerosol sources in Paris using high resolution aerosol mass spectrometry, J. Geophys. Res., 118, 1950–1963, https://doi.org/10.1002/jgrd.50151, 2013b.

Daher, N., Saleh, R., Jaroudi, E., Sheheitli, H., Badr, T., Sepetdjian, E., Al Rashidi, M., Saliba, N., and Shihadeh, A.: Comparison of carcinogen, carbon monoxide, and ultrafine particle emissions from narghile waterpipe and cigarette smoking: Sidestream smoke measurements and assessment of second-hand smoke emission factors, Atmospheric Environment, 44, 8–14, https://doi.org/10.1016/j.atmosenv.2009.10.004, 2010.

Derudi, M., Gelosa, S., Sliepcevich, A., Cattaneo, A., Cavallo, D., Rota, R., and Nano, G.: Emission of air pollutants from burning candles with different composition in indoor environments, Environmental Science and Pollution Research, 21, 4320–4330, https://doi.org/10.1007/s11356-013-2394-2, 2014.

Docherty, K. S., Aiken, A. C., Huffman, J. A., Ulbrich, I. M., DeCarlo, P. F., Sueper, D., Worsnop, D. R., Snyder, D. C., Peltier, R. E., Weber, R. J., Grover, B. D., Eatough, D. J., Williams, B. J., Goldstein, A. H., Ziemann, P. J., and Jimenez, J. L.: The 2005 Study of Organic Aerosols at Riverside (SOAR-1): instrumental intercomparisons and fine particle composition, Atmos. Chem. Phys., 11, 12387–12420, https://doi.org/10.5194/acp-11-12387-2011, 2011.

Drewnick, F., Böttger, T., Weiden-Reinmüller, S.-L. v. d., Zorn, S. R., Klimach, T., Schneider, J., and Borrmann, S.: Design of a mobile aerosol research laboratory and data processing tools for effective stationary and mobile field measurements, Atmos. Meas. Tech., 5, 1443–1457, https://doi.org/10.5194/amt-5-1443-2012, 2012.

Elser, M., Huang, R.-J., Wolf, R., Slowik, J. G., Wang, Q., Canonaco, F., Li, G., Bozzetti, C., Daellenbach, K. R., Huang, Y., Zhang, R., Li, Z., Cao, J., Baltensperger, U., El-Haddad, I., and Prévôt, A. S. H.: New insights into $PM_{2.5}$ chemical composition and sources in two major cities in China during extreme haze events using aerosol mass spectrometry, Atmos. Chem. Phys., 16, 3207–3225, https://doi.org/10.5194/acp-16-3207-2016, 2016.

Endo, O., Koyano, M., Mineki, S., Goto, S., Tanabe, K., Yajima, H., Ishii, T., and Matsushita, H.: Estimation of Indoor Air PAH Concentration Increases by Cigarette, Incense-Stick, and Mosquito-Repellent-Incense Smoke, Polycyclic Aromatic Compounds, 21, 261–272, https://doi.org/10.1080/10406630008028538, 2000.

Fachinger, F., Drewnick, F., Gieré, R., and Borrmann, S.: How the user can influence particulate emissions from residential wood and pellet stoves: Emission factors for different fuels and burning conditions, Atmospheric Environment, 158, 216–226, https://doi.org/10.1016/j.atmosenv.2017.03.027, 2017.

Freutel, F., Schneider, J., Drewnick, F., Weiden-Reinmüller, S.-L. v. d., Crippa, M., Prévôt, A. S. H., Baltensperger, U., Poulain, L., Wiedensohler, A., Sciare, J., Sarda-Estève, R., Burkhart, J. F., Eckhardt, S., Stohl, A., Gros, V., Colomb, A., Michoud, V., Doussin, J. F., Borbon, A., Haeffelin, M., Morille, Y., Beekmann, M., and Borrmann, S.: Aerosol particle measurements at three stationary sites in the megacity of Paris during summer 2009: meteorology and air mass origin dominate aerosol particle composition and size distribution, Atmos. Chem. Phys., 13, 933–959, https://doi.org/10.5194/acp-13-933-2013, 2013.

Hayes, P. L., Ortega, A. M., Cubison, M. J., Froyd, K. D., Zhao, Y., Cliff, S. S., Hu, W. W., Toohey, D. W., Flynn, J. H., Lefer, B. L., Grossberg, N., Alvarez, S., Rappenglück, B., Taylor, J. W., Allan, J. D., Holloway, J. S., Gilman, J. B., Kuster, W. C., Gouw, J. A. de, Massoli, P., Zhang, X., Liu, J., Weber, R. J., Corrigan, A. L., Russell, L. M., Isaacman, G., Worton, D. R., Kreisberg, N. M., Goldstein, A. H., Thalman, R., Waxman, E. M., Volkamer, R., Lin, Y. H., Surratt, J. D., Kleindienst, T. E., Offenberg, J. H., Dusanter, S., Griffith, S., Stevens, P. S., Brioude, J., Angevine, W. M., and Jimenez, J. L.: Organic aerosol composition and sources in Pasadena, California, during the 2010 CalNex campaign, J. Geophys. Res. Atmos., 118, 9233–9257, https://doi.org/10.1002/jgrd.50530, 2013.

Hearn, B. A., Ding, Y. S., Watson, C. H., Johnson, T. L., Zewdie, G., Jeong-Im, J. H., Walters, M. J., Holman, M. R., and Rochester, C. G.: Multi-year Study of PAHs in Mainstream Cigarette Smoke, Tobacco Regulatory Science, 4, 96–106, https://doi.org/10.18001/trs.4.3.9, 2018.

Hersey, S. P., Craven, J. S., Schilling, K. A., Metcalf, A. R., Sorooshian, A., Chan, M. N., Flagan, R. C., and Seinfeld, J. H.: The Pasadena Aerosol Characterization Observatory (PACO): chemical and physical analysis of the Western Los Angeles basin aerosol, Atmos. Chem. Phys., 11, 7417–7443, https://doi.org/10.5194/acp-11-7417-2011, 2011.

Hinds, W. C.: Aerosol Technology: Properties, Behavior, and Measurement of Airborne Particles, 2nd ed., John Wiley & Sons, Inc., Hoboken, 464 pp., 1999.

Hu, W. W., Campuzano-Jost, P., Palm, B. B., Day, D. A., Ortega, A. M., Hayes, P. L., Krechmer, J. E., Chen, Q., Kuwata, M., Liu, Y. J., Sá, S. S. de, McKinney, K., Martin, S. T., Hu, M., Budisulistiorini, S. H., Riva, M., Surratt, J. D., St. Clair, J. M., Isaacman-Van Wertz, G., Yee, L. D., Goldstein, A. H., Carbone, S., Brito, J., Artaxo, P., Gouw, J. A. de, Koss, A., Wisthaler, A., Mikoviny, T., Karl, T., Kaser, L., Jud, W., Hansel, A., Docherty, K. S., Alexander, M. L., Robinson, N. H., Coe, H., Allan, J. D., Canagaratna, M. R., Paulot, F., and Jimenez, J. L.: Characterization of a real-time tracer for isoprene epoxydiols-derived secondary organic aerosol (IEPOX-SOA) from aerosol mass spectrometer measurements, Atmos. Chem. Phys., 15, 11807–11833, https://doi.org/10.5194/acp-15-11807-2015, 2015.

Hu, W. W., Hu, M., Yuan, B., Jimenez, J. L., Tang, Q., Peng, J. F., Hu, W., Shao, M., Wang, M., Zeng, L. M., Wu, Y. S., Gong, Z. H., Huang, X. F., and He, L. Y.: Insights on organic aerosol aging and the influence of coal combustion at a regional receptor site of central eastern China, Atmos. Chem. Phys., 13, 10095–10112, https://doi.org/10.5194/acp-13-10095-2013, 2013.

Hu, W., Day, D. A., Campuzano-Jost, P., Nault, B. A., Park, T., Lee, T., Croteau, P., Canagaratna, M. R., Jayne, J. T., Worsnop, D. R., and Jimenez, J. L.: Evaluation of the New Capture Vaporizer for Aerosol Mass Spectrometers (AMS): Elemental Composition and Source Apportionment of Organic Aerosols (OA), ACS Earth Space Chem., 2, 410–421, https://doi.org/10.1021/acsearthspacechem.8b00002, 2018.

Hu, W., Hu, M., Hu, W., Jimenez, J. L., Yuan, B., Chen, W., Wang, M., Wu, Y., Chen, C., Wang, Z., Peng, J., Zeng, L., and Shao, M.: Chemical composition, sources, and aging process of submicron aerosols in Beijing: Contrast between summer and winter, J. Geophys. Res. Atmos., 121, 1955–1977, https://doi.org/10.1002/2015JD024020, 2016.

Johansson, L. S., Leckner, B., Gustavsson, L., Cooper, D., Tullin, C., and Potter, A.: Emission characteristics of modern and old-type residential boilers fired with wood logs and wood pellets, Atmospheric Environment, 38, 4183–4195, https://doi.org/10.1016/j.atmosenv.2004.04.020, 2004.

Katz, E. F., Guo, H., Campuzano-Jost, P., Day, D. A., Brown, W. L., Boedicker, E., Pothier, M., Lunderberg, D. M., Patel, S., Patel, K., Hayes, P. L., Avery, A., Hildebrandt Ruiz, L., Goldstein, A. H., Vance, M. E., Farmer, D. K., Jimenez, J. L., and DeCarlo, P. F.: Quantification of cooking organic aerosol in the indoor environment using aerodyne aerosol mass spectrometers, Aerosol Sci. Technol., 55, 1099–1114, https://doi.org/10.1080/02786826.2021.1931013, 2021.

Kuwata, M., Zorn, S. R., and Martin, S. T.: Using elemental ratios to predict the density of organic material composed of carbon, hydrogen, and oxygen, Environ. Sci. Technol., 46, 787–794, https://doi.org/10.1021/es202525q, 2012.

Levin, E. J. T., McMeeking, G. R., Carrico, C. M., Mack, L. E., Kreidenweis, S. M., Wold, C. E., Moosmüller, H., Arnott, W. P., Hao, W. M., Collett, J. L., and Malm, W. C.: Biomass burning smoke aerosol properties measured during Fire Laboratory at Missoula Experiments (FLAME), J. Geophys. Res., 115, https://doi.org/10.1029/2009jd013601, 2010.

Mohr, C., DeCarlo, P. F., Heringa, M. F., Chirico, R., Slowik, J. G., Richter, R., Reche, C., Alastuey, A., Querol, X., Seco, R., Peñuelas, J., Jiménez, J. L., Crippa, M., Zimmermann, R., Baltensperger, U., and Prévôt, A. S. H.: Identification and quantification of organic aerosol from cooking and other sources in Barcelona using aerosol mass spectrometer data, Atmos. Chem. Phys., 12, 1649–1665, https://doi.org/10.5194/acp-12-1649-2012, 2012.

Pagels, J., Wierzbicka, A., Nilsson, E., Isaxon, C., Dahl, A., Gudmundsson, A., Swietlicki, E., and Bohgard, M.: Chemical composition and mass emission factors of candle smoke particles, Journal of Aerosol Science, 40, 193–208, https://doi.org/10.1016/j.jaerosci.2008.10.005, 2009.

Pikmann, J., Moormann, L., Drewnick, F., and Borrmann, S.: The AERosol and TRACe gas Collector (AERTRACC): an online measurement controlled sampler for source-resolved emission analysis, Atmos. Meas. Tech., https://doi.org/10.5194/amt-2022-206, 2022.

Reitz, P.: Chemical Composition Measurements of Cloud Condensation Nuclei and Ice Nuclei by Aerosol Mass Spectrometry, Dissertation, Johannes Gutenberg-Universität Mainz, Mainz, 2011.

Reyes-Villegas, E., Bannan, T., Le Breton, M., Mehra, A., Priestley, M., Percival, C., Coe, H., and Allan, J. D.: Online chemical characterization of food-cooking organic aerosols: Implications for source apportionment, Environ. Sci. Technol., 52, 5308–5318, https://doi.org/10.1021/acs.est.7b06278, 2018.

Rumble, J. R.: CRC Handbook of Chemistry and Physics, (Internet Version 2022), 103rd ed., CRC Press/Taylor & Francis, Boca Raton, Florida, 2022.

Ruprecht, A. A., Marco, C. de, Saffari, A., Pozzi, P., Mazza, R., Veronese, C., Angellotti, G., Munarini, E., Ogliari, A. C., Westerdahl, D., Hasheminassab, S., Shafer, M. M., Schauer, J. J., Repace, J., Sioutas, C., and Boffi, R.: Environmental pollution and emission factors of electronic cigarettes, heat-not-burn tobacco products, and conventional cigarettes, Aerosol Science and Technology, 51, 674–684, https://doi.org/10.1080/02786826.2017.1300231, 2017.

Saarikoski, S., Carbone, S., Decesari, S., Giulianelli, L., Angelini, F., Canagaratna, M., Ng, N. L., Trimborn, A., Facchini, M. C., Fuzzi, S., Hillamo, R., and Worsnop, D.: Chemical characterization of springtime submicrometer aerosol in Po Valley, Italy, Atmos. Chem. Phys., 12, 8401–8421, https://doi.org/10.5194/acp-12-8401-2012, 2012.

Salcedo, D., Onasch, T. B., Dzepina, K., Canagaratna, M. R., Zhang, Q., Huffman, J. A., DeCarlo, P. F., Jayne, J. T., Mortimer, P., Worsnop, D. R., Kolb, C. E., Johnson, K. S., Zuberi, B., Marr, L. C., Volkamer, R., Molina, L. T., Molina, M. J., Cardenas, B., Bernabé, R. M., Márquez, C., Gaffney, J. S., Marley, N. A., Laskin, A., Shutthanandan, V., Xie, Y., Brune, W., Lesher, R., Shirley, T., and Jimenez, J. L.: Characterization of ambient aerosols in Mexico City during the

MCMA-2003 campaign with Aerosol Mass Spectrometry: results from the CENICA Supersite, Atmos. Chem. Phys., 6, 925–946, https://doi.org/10.5194/acp-6-925-2006, 2006.

Savdie, J., Canha, N., Buitrago, N., and Almeida, S. M.: Passive Exposure to Pollutants from a New Generation of Cigarettes in Real Life Scenarios, International Journal of Environmental Research and Public Health, 17, https://doi.org/10.3390/ijerph17103455, 2020.

Seinfeld, J. H. and Pandis, S. N.: Atmospheric Chemistry and Physics: From Air Pollution to Climate Change, 2nd ed., Wiley-Interscience, New York, 464 pp., 2006.

Setyan, A., Zhang, Q., Merkel, M., Knighton, W. B., Sun, Y., Song, C., Shilling, J. E., Onasch, T. B., Herndon, S. C., Worsnop, D. R., Fast, J. D., Zaveri, R. A., Berg, L. K., Wiedensohler, A., Flowers, B. A., Dubey, M. K., and Subramanian, R.: Characterization of submicron particles influenced by mixed biogenic and anthropogenic emissions using high-resolution aerosol mass spectrometry: results from CARES, Atmos. Chem. Phys., 12, 8131–8156, https://doi.org/10.5194/acp-12-8131-2012, 2012.

Shen, G., Tao, S., Wei, S., Zhang, Y., Wang, R., Wang, B., Li, W., Shen, H., Huang, Y., Chen, Y., Chen, H., Yang, Y., Wang, W., Wei, W., Wang, X., Liu, W., Wang, X., and Masse Simonich, S. L.: Reductions in emissions of carbonaceous particulate matter and polycyclic aromatic hydrocarbons from combustion of biomass pellets in comparison with raw fuel burning, Environmental Science & Technology, 46, 6409–6416, https://doi.org/10.1021/es300369d, 2012.

Stabile, L., Fuoco, F. C., and Buonanno, G.: Characteristics of particles and black carbon emitted by combustion of incenses, candles and anti-mosquito products, Building and Environment, 56, 184–191, https://doi.org/10.1016/j.buildenv.2012.03.005, 2012.

Struckmeier, C., Drewnick, F., Fachinger, F., Gobbi, G. P., and Borrmann, S.: Atmospheric aerosols in Rome, Italy: sources, dynamics and spatial variations during two seasons, Atmos. Chem. Phys., 16, 15277–15299, https://doi.org/10.5194/acp-16-15277-2016, 2016.

Tang, I. N.: Chemical and size effects of hygroscopic aerosols on light scattering coefficients, J. Geophys. Res., 101, 19245–19250, https://doi.org/10.1029/96JD03003, 1996.

Ulbrich, I. M., Canagaratna, M. R., Zhang, Q., Worsnop, D. R., and Jimenez, J. L.: Interpretation of organic components from Positive Matrix Factorization of aerosol mass spectrometric data, Atmos. Chem. Phys., 9, 2891–2918, https://doi.org/10.5194/acp-9-2891-2009, 2009.

Ulbrich, I. M., Handschy, A., Lechner, M., and Jimenez, J.L.: High-Resolution AMS Spectral Database, http://cires.colorado.edu/jimenez-group/HRAMSsd/, last access: 18 September 2023.

Vetter, T.: Berechnung der Mie-Streufunktionen zur Kalibrierung optischer Partikelzähler, Diploma thesis, Institut für Physik der Atmosphäre, Johannes Gutenberg-Universität Mainz und Abteilung Wolkenphysik und -chemie, Johannes Gutenberg-Universität Mainz, Mainz, 2004.

Wallace, L. and Ott, W.: Personal exposure to ultrafine particles, J. Expo. Sci. Environ. Epidemiol., 21, 20–30, https://doi.org/10.1038/jes.2009.59, 2011.

Zai, S., Zhen, H., and Jia-song, W.: Studies on the size distribution, number and mass emission factors of candle particles characterized by modes of burning, Journal of Aerosol Science, 37, 1484–1496, https://doi.org/10.1016/j.jaerosci.2006.05.001, 2006.